Available online at www.sciencedirect.com
ScienceDirect
Journal of Hazardous Materials 155 (2008) 100–108
Journal of Hazardous Materials
www.elsevier.com/locate/jhazmat

Synthesis of magnetic chelating resins functionalized with tetraethylenepentamine for adsorption of molybdate anions from aqueous solutions

Asem A. Atia, Ahmed M. Donia *, Haytham A. Awed

Chemistry Department, Faculty of Science, Menoufia University, Shebin El-Kom, Egypt

Received 29 August 2007; received in revised form 13 November 2007; accepted 13 November 2007
Available online 19 November 2007

Abstract

Magnetic resins were synthesized through polymerization of glycidyl methacrylate (GMA) in the presence of divinylbenzene (DVB) or *N*,*N*′-methylenebisacrylamide (MBA) as hydrophobic or hydrophilic crosslinker, respectively and in presence of suspended magnetite particles. The resins containing (DVB or MBA) as crosslinker were immobilized with tetraethylenepentamine (TEP) to give the amino resins, GMA/DVB/TEP (R1-en) and GMA/MBA/TEP (R2-en), respectively. The uptake behavior of the two resins was studied towards molybdate anions and uptake capacities of 4.24 and 6.18 mmol/g [as (Mo(VI)] were obtained using (R1-en) and (R2-en). Kinetic studies showed that the adsorption followed the pseudo-second-order model pointing the influence of the textural properties of the resin on the rate of adsorption. Thermodynamic data indicated an endothermic adsorption process. The uptake of Mo(VI) and regeneration of the resins were also studied using the column method. Regeneration efficiency up to 90–96% was reached using ammonia buffer.

Keywords: Molybdate; Magnetic resins; Glycidyl methacrylate; Adsorption; Kinetics; Thermodynamics

1. Introduction

Molybdenum is essential for some biological functions in plants and animals [1]. It is the most concentrated trace element in the seawater due to its stability and weak adsorption behavior [2]. Its compounds exhibit all oxidation states from 2+ to 6+ with the predominant states Mo(IV) and Mo(VI) [3]. Molybdenum and its compounds are essentially used in alloys production and as inhibitors for steel corrosion due to their low toxicity [4,5]. High concentrations of molybdate (more than 5 ppm) cause environmental problem [6]. For example, the increase in molybdenum levels in human body cause diseases such as anemia, bone and joint deformities, liver and kidney abnormalities and finally death [7]. So, the removal of molybdenum ion from wastewater and ground water becomes of great significance from the environmental point of view. The removal of molybdate has been achieved by various methods such as co-precipitation and reverse osmosis. These methods generally need different reagents and complicated facilities [8–10]. Adsorption is a simple and facile technique used in molybdate treatment. Different adsorbents such as pyrite, kaolinite, natrolite, titania, iron oxide, aluminum oxide, etc. were used for molybdate removal from aqueous solutions [11–17]. Growing attention has recently been given to chelating resins due to their relatively fast removal rates and selectivity towards trace elements [18–23]. Glycidyl methacrylate based chelating resins have various applications in the field of separation and preconcentration of pollutants [24–27]. Special interest has also been given to magnetic chelating resins due to their high uptake capacity and easy of collection using an external magnetic field [28–31]. In this work, magnetic chelating resins of glycidyl methacrylate with different crosslinkers and pentamine functionality have been prepared and used for removal of molybdate anion from aqueous solutions. The removal process has also been investigated at different experimental conditions of time, pH, initial concentration of adsorbate and temperature. The mechanism

* Corresponding author.
E-mail addresses: asemali2010@yahoo.com (A.A. Atia), ahmeddonia2003@yahoo.com (A.M. Donia), hythamawed@yahoo.com (H.A. Awed).

0304-3894/$ – see front matter © 2007 Published by Elsevier B.V.
doi:10.1016/j.jhazmat.2007.11.035

of interaction between the active sites and molybdate anion as well as the thermodynamic and kinetics properties of adsorption process will also be clarified.

2. Experimental

2.1. Chemicals

Glycidyl methacrylate (GMA), *N*,*N*′-methylenebisacrylamide (MBA), divinylbenzene (DVB, 55%), benzoyl peroxide (Bz_2O_2), tetraethylenepentamine (TEP) were Aldrich products. All other chemicals were of analytical grade and were used as received. $FeSO_4.7H_2O$, $FeCl_3.6H_2O$ and $(NH_4)_6Mo_7O_{24}.4H_2O$ were used as sources for Fe(II), Fe(III) and Mo(VI), respectively.

2.2. Preparation of magnetite

Magnetite was prepared following the modified Massart method [32]. A 250 mL (0.2 M) of Fe(III) solution was added with stirring to a freshly prepared 250 mL (1.2 M) of Fe(II) solution. A 200 mL of ammonia solution (30%) was suddenly poured to the previously prepared Fe(III)/Fe(II) solution while vigorous stirring. A black precipitate was formed and was allowed to crystallize for 30 min with stirring. The precipitate was washed with deoxygenated water (water was boiled to repeal any gases then bubbled with nitrogen gas) under magnetic decantation until the acidity of suspension became below pH 7.5. The precipitate was dried at room temperature to give a black powder.

2.3. Preparation of magnetic resins

GMA/DVB-magnetite (R1) and GMA/MBA-magnetite (R2) resins were prepared through polymerization of GMA in the presence of suspended magnetite particles and DVB or MBA as a crosslinker. A mixture of 9.5 mL GMA and 0.5 mL DVB or 0.5 g MBA was prepared. A 0.1 g Bz_2O_2 (initiator) was added to the above mixture with stirring. One milliliter of isopropyl alcohol and 12.6 mL of cyclohexane were also mixed and then added to the solution. All the contents were poured into a flask containing 73 mL (1%) poly(vinyl alcohol) then 1.0 g powdered Fe_3O_4 was added and refluxed on a water bath at 75–80 °C with continuous stirring for 3 h. A heavy grayish precipitate was formed, filtered off, washed with methanol and then dried in air [29].

2.4. Immobilization of the resins by tetraethylenepentamine

The magnetic resins obtained in the previous step (R1 and R2) were loaded by tetraethylenepentamine as follows: 1 g of the resin was suspended in 3 mL of amine dissolved in 12 mL DMF. The reaction mixture was heated up to 75–80 °C for 72 h on an oil bath. The products obtained were filtered off, washed with methanol and then dried in air and referred as R1-en and R2-en [31].

2.5. Estimation of amino groups

The concentration of amino group on the resins was estimated using the volumetric method [23]. Forty milliliters of 0.05 N HCl solution was added to 0.1 g resin and conditioned for 15 h on a shaker. The number of moles of HCl was measured through the titration against 0.05 N NaOH solution and phenolphthalein as indicator. The number of moles of HCl interacting with the amino groups were calculated and consequently the amino group concentration (in mmol/g of resin) was calculated using the following equation:

$$\text{Concentration of}(NH_2)\text{group} = \frac{(M_1 - M_2) \times 40}{0.1}(\text{mmol/g of resin}) \quad (1)$$

where M_1 and M_2 are the initial and final concentrations of HCl.

3. Uptake measurements

3.1. Batch method

Effect of contact time on the uptake of molybdate anions by resins (R1-en and R2-en) was carried out by placing 0.1 g of dry resin in a flask containing 100 mL of Mo(VI) at initial concentration of 8×10^{-3} M and pH 2. The contents of the flask were equilibrated on a Vibromatic-384 shaker at 300 rpm and 28 °C. Five milliliters of the solution were taken at different time intervals where the residual concentration of molybdate anion was determined. The absorbance was measured at 420 nm using mercaptoacetic method [33].

Adsorption of molybdate anion on the resins under controlled pH was carried out following the above procedures. The desired pH was adjusted using HCL while the equilibrium time was fixed at 3 h and 28 °C.

Complete adsorption isotherms were obtained at pH 2 and at different temperatures. A 0.1 g of dry resin was conditioned with 100 mL molybdate solution with different concentrations for 3 h and at 28, 40, 50 and 60 °C. The residual concentration of molybdate was estimated.

3.2. Column experiments

Column experiments were performed in a plastic column length of 10 cm and a diameter of 1.0 cm. A small amount of glass wool was placed at the bottom of the column to keep the contents. A known quantity of the resin under investigation was placed in the column to yield the desired bed height. Molybdate anion solution of initial concentration 3×10^{-3} M was flowed downward through the column at a desired flow rate. Samples were collected from the outlet of the column at different time intervals and analyzed for metal ion concentration. The operation of the column was stopped when the outlet metal ion concentration matched its initial concentration. The outlet metal ion concentrations were plotted versus time at different flow rates to give the breakthrough curves.

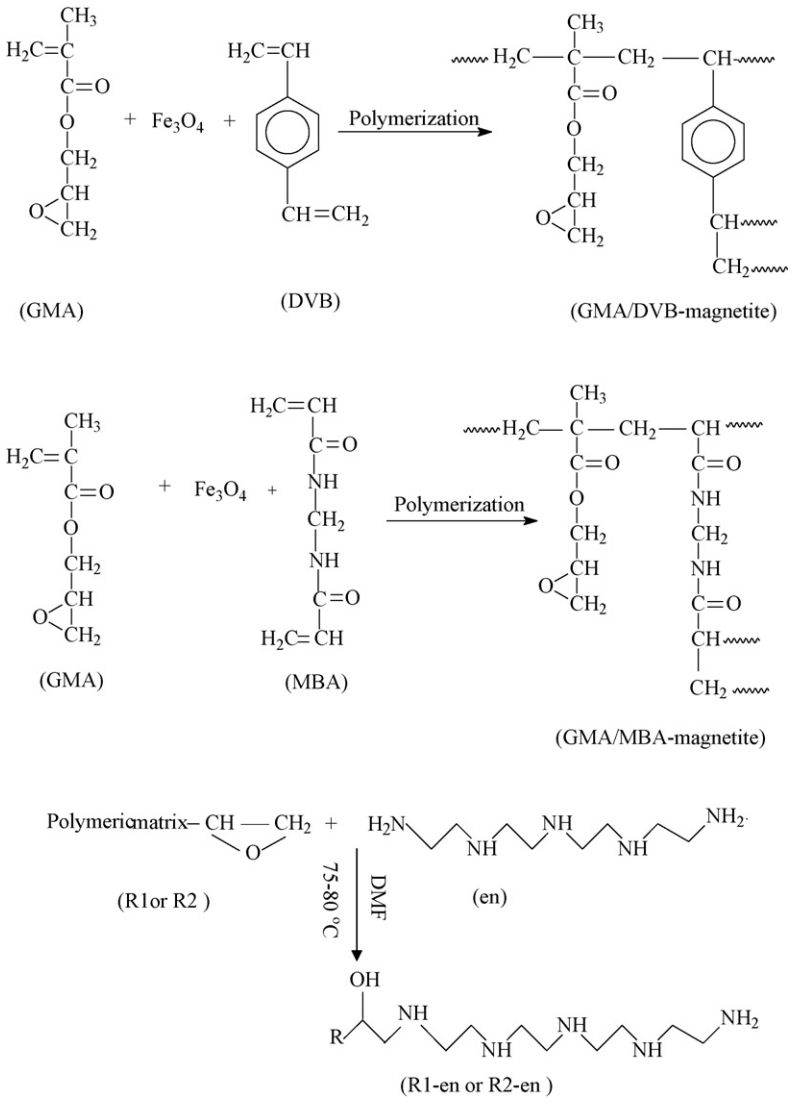

Scheme 1. Synthetic routes of resins.

3.3. Resin regeneration

Regeneration experiments were performed by placing 0.5 g of resin in the column and then loaded with molybdate anion at flow rate 1 mL/min. After reaching the maximum uptake in the first run, the resin was washed carefully by flowing distilled water through the column. The resin loaded by molybdate anion was then subjected for elution using a mixture of 0.1 M ammonium hydroxide and 0.01 M ammonium chloride. Afterwards the resin was again carefully washed with distilled water to make it ready for the second run of uptake. The efficiency of elution was calculated using the following equation:

$$\text{Elution effiency}(\%) = \frac{\text{Total adsorption capacity in second run}}{\text{Total adsorption capacity in the first run}} \times 100 \quad (2)$$

4. Results and discussions

The synthesis process of the resins is presented in Scheme 1. The structural formula of the resins obtained was confirmed from IR spectra. The spectra of resins R1 and R2 showed the stretching band of oxirane group at 910 cm^{-1}. This band disappeared in the spectra of their corresponding amine (R1-en) and (R2-en). Moreover, the spectra of (R1-en) and (R2-en) are characterized by νNH_2 at 3743 cm^{-1}. This indicates the success of modification process. The resin particle size of 4 μm was used in the adsorption studies.

4.1. Effect of pH

The adsorption of molybdate anion on resins (R1-en) and (R2-en) as a function of pH is shown in Fig. 1. The uptake

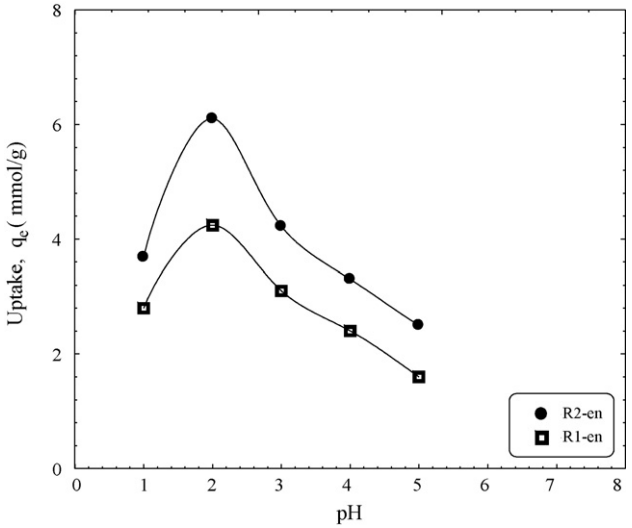

Fig. 1. Effect of pH on the uptake of molybdate anion by studied resins at initial concentration 8×10^{-3} M; contact time 3 h; 28 °C.

capacity showed a maximum value at pH 2 for both resins. The uptake value decreased in stronger acidic or basic media, i.e. pH < 2 or pH > 2. The adsorption of molybdate on the studied resins may be interpreted based on the surface charge of the resin and on the type of the existing molybdenum ion species. Molybdenum in aqueous solutions exists in various hydrolytic species depending on the total metal concentration and pH. The most probable molybdate species present in aqueous solutions are $[Mo_7O_{21}(OH)_3]^{3-}$, $[Mo_7O_{22}(OH)_2]^{4-}$, $[Mo_7O_{23}(OH)_5]^{5-}$ and $[Mo_7O_{24}]^{6-}$ [7]. At pH > 6, the tetrahedral monomeric molybdate ion (MoO_4^{2-}) exists. This anion can be protonated at low pH values forming H_2MoO_4. At pH < 6 (at concentrations above 1×10^{-4} M) the heptamolybdate polyanion $Mo_7O_{24}^{6-}$ exists. The heptamolybdate can be singly, doubly or even triply protonated [15]. So, the maximum uptake of molybdate at pH 2 may be explained to proceed through ion exchange mechanism at the protonated amino active sites as follows:

$$\text{R-N} + \text{HCl} \leftrightarrow \text{RNH}^+\text{Cl}^- \quad (3)$$

$$6\text{RNH}^+\text{Cl}^- + \text{Mo}_7\text{O}_{24}^{6-} \leftrightarrow 6\text{RNHMo}_7\text{O}_{24}^{6-} + 6\text{Cl}^- \quad (4)$$

At pH < 2, the decrease in adsorption capacity may be attributed to the competitive adsorption between Cl^- anions (with higher concentration) and molybdate anion ($Mo_7O_{24}^{6-}$). The observed decrease in the adsorption capacity above pH 2 may be attributed to the partial deprotonation of the amino group which leads to the decrease of uptake value.

4.2. Adsorption isotherms

Fig. 2 shows the adsorption isotherms of molybdate anions by (R1-en) and (R2-en) at pH 2 and at different temperatures. Generally as the temperature increases the uptake value increases. This behavior may be attributed to: (i) The increase of active site number due to the more flexible resin framework on increasing the temperature; (ii) the less dehydration of the active sites as well as the molybdate anions at elevated temperatures facilitating better interaction [34]. The maximum uptake values of molybdate anions were found to be 4.24 and 6.18 mmol/g at 28 °C for (R1-en) and (R2-en), respectively. These values are much lower than the concentration of amino group on the resins (11.8 and 17.0 mmol/g for R1-en and R2-en, respectively). This may be attributed to the large size of molybdate anion ($Mo_7O_{24}^{6-}$) relative to H^+. The higher value of uptake in the case of (R2-en) relative to that of (R1-en) may be attributed to the hydrophilic nature of (MBA) relative to hydrophobic (DVB). The hydrophilic crosslinker facilitates the approach of $Mo_7O_{24}^{6-}$ to the resin's surface giving efficient binding with active sites. The data given in Fig. 2 were treated according to the following Langmuir equation:

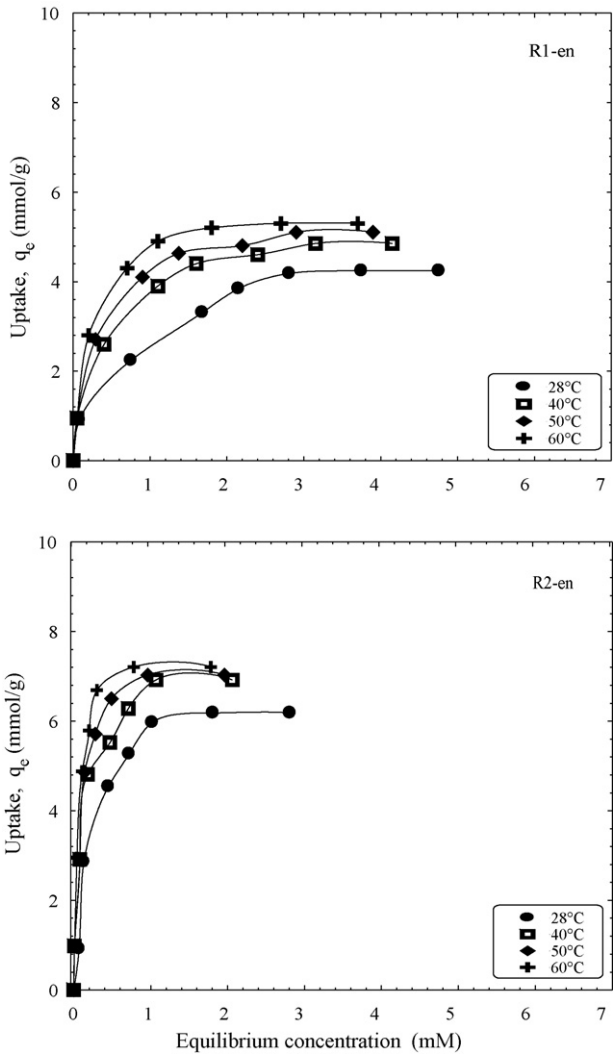

Fig. 2. Adsorption isotherm of molybdate anion on resins at different temperatures; pH 2; contact time 3 h.

$$\frac{C_e}{q_e} = \frac{C_e}{Q_{max}} + \frac{1}{K_{ads} Q_{max}}. \quad (5)$$

where C_e is the equilibrium concentration of metal ions in solution (mmol/L), q_e is the adsorbed value of metal ions at equilibrium concentration (mmol/g), Q_{max} is the maximum adsorption capacity (mmol/g), and K_{ads} is the binding constant

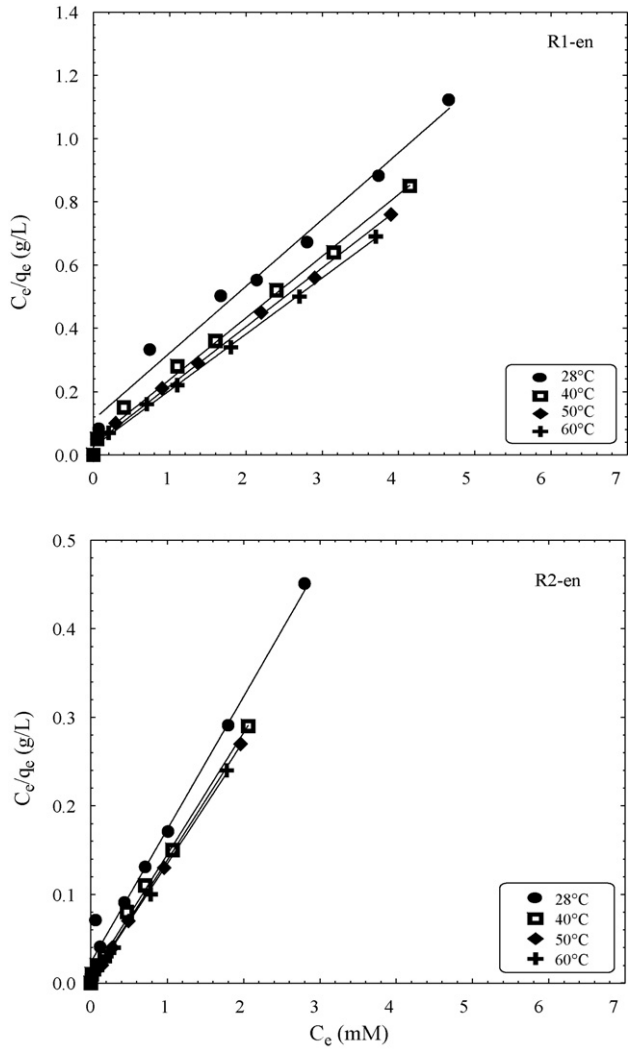

Fig. 3. Langmuir plots for the adsorption of molybdate anion on resins at different temperature.

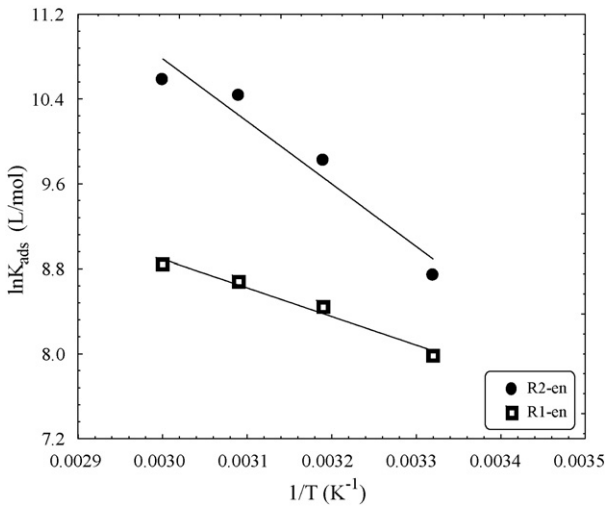

Fig. 4. Van't Hoff plot for adsorption of molybdate anion on resins.

which is related to the energy of adsorption (L/mmol). Plotting C_e/q_e against C_e gives a straight line with slope and intercept equal $1/Q_{max}$ and $1/K_{ads}Q_{max}$, respectively. The values of K_{ads} and Q_{max} at different temperatures were obtained from Fig. 3 and reported in Table 1. The values of Q_{max} are comparable with the experimental ones. At all temperatures the K_{ads} values of R2-en are greater than those of R1-en. This again reflects the higher binding of molybdate anion with the hydrophilic surface of resin (R2-en) compared to (R1-en). On the other hand, for both resins the observed increase in K_{ads} values with temperature may be related to the partial dehydration of active sites more efficient in electrostatic interaction [35]. Thermodynamic parameters of adsorption reaction were calculated from the following van't Hoff equation [36]:

$$\ln K_{ads} = \frac{-\Delta H^\circ}{RT} + \frac{\Delta S^\circ}{R} \quad (6)$$

where ΔH° and $\Delta S^\circ$are the enthalpy and entropy changes, R is the universal gas constant (8.314 J/mol K) and T is the absolute temperature (K). Plotting $\ln K_{ads}$ against $1/T$ gives a straight line with slope and intercept equal to $-\Delta H^\circ/R$ and $\Delta S^\circ/R$, respectively. The values of ΔH° and ΔS° were calculated from Fig. 4 and reported in Table 2. The positive value of ΔH° indicates an endothermic adsorption process. The positive values of ΔS° may be related to the randomness obtained from the destructive of the hydration spheres of both active site and molybdate anion. The data given in Table 2 also show that $|\Delta H^\circ| < |T\Delta S^\circ|$at all temperatures. This indicates that the adsorption process is controlled by entropic rather than enthalpic changes [36]. The Gibbs free energy of adsorption (ΔG°) was calculated from the following relation:

$$\Delta G^\circ = \Delta H^\circ - T\Delta S^\circ \quad (7)$$

The values obtained of ΔG° and $T\Delta S^\circ$ are also given in Table 2. The negative values of ΔG° indicate a spontaneous adsorption process. The observed increase in the negative value

Table 1
Values of Langmuir parameters for the adsorption of molybdate anion on resins at different temperatures

Temperature (°C)	R1-en			R2-en		
	Q_{max} (mmol/g)		K_{ads} (L/mmol)	Q_{max} (mmol/g)		K_{ads} (L/mmol)
	Exp.	Theo.		Exp.	Theo.	
28	4.24	4.50	2.9	6.18	6.60	6.3
40	4.80	5.10	4.6	6.92	7.20	18.3
50	5.10	5.30	5.9	7.03	7.40	34.1
60	5.30	5.60	6.9	7.21	7.60	38.9

Table 2
Thermodynamic parameters of the adsorption of molybdate anion on resins

Resin	ΔH^o(kJ/mol)	ΔS^o (kJ/mol K)	Temperature (K)	ΔG^o (kJ/mol)	$T\Delta S^o$ (kJ/mol)
R1-en	22.40	0.14	301	−19.74	42.11
			313	−21.42	43.83
			323	−22.82	45.22
			333	−24.22	46.62
R2-en	49.06	0.23	301	−20.17	69.23
			313	−20.93	71.99
			323	−25.23	74.29
			333	−27.53	76.59

of ΔG° with increasing temperature implies that the adsorption becomes more favorable at higher temperature.

4.3. Kinetic studies

The effect of contact time on the adsorption of molybdate anion at initial concentration of 8×10^{-3} M. The investigated resins at 28 °C and pH 2 is shown in Fig. 5 Obviously, the rate of uptake was fast within 30 min. Values of 66 and 86% of the maximum uptakes were achieved by R1-en and R2-en, respectively. The maximum uptake was reached within 3 h. The uptake/time data shown in Fig. 5 were treated according the pseudo-second-order model [37]:

$$\frac{t}{q_t} = \frac{1}{k_2 q_e^2} + \frac{1}{q_e} t \tag{8}$$

where q_e and q_t refer to the amount of molybdate anion adsorbed (mmol/g) at equilibrium and at any time, t (min), respectively, and k_2 is the equilibrium rate constant of pseudo-second-order adsorption (g mmol^{-1} min^{-1}). The linear plots of t/q_t versus t (Fig. 6) gave straight line with intercept and slope equal to $(1/q_e)$ and $(1/k_2 q_e^2)$ from which the values of k_2 and q_e were calculated and reported in Table 3. Values of q_e for (R1-en) and (R2-en) are in good agreement with the experimental ones. This indicates the validity of the pseudo-second-order model to describe the kinetic of process. The relatively lower value of the rate constant (k_2) in case of (R1-en) compared to that of (R2-en) may be attributed to the lower hydrophilicity of (R1-en). The relationship between the uptake and the square root of time indicates the effect of the intraparticle diffusion on the rate of reaction. The rate of intraparticle diffusion can be described as [38]:

$$q_t = K_{id} t^{0.5} \tag{9}$$

where K_{id} is intraparticle diffusion rate (mmol/g min$^{-0.5}$). The K_{id} is the slope of straight-line portions of the plot of q_t versus $t^{0.5}$ (Fig. 7). The K_{id} values were calculated and found to be 0.43 and 0.66 (mmol/g min$^{-0.5}$) for R1-en and R2-en, respectively. The higher value of K_{id} refers to faster intraparticle diffusion in the case of R2-en relative to R1-en due to the hydrophilicity of the former.

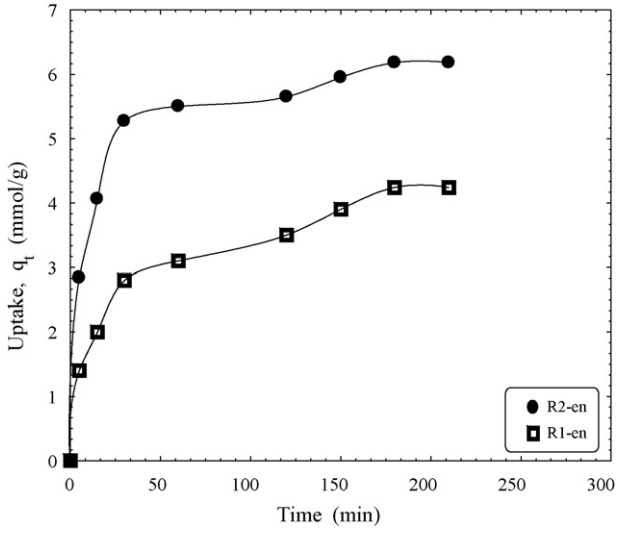

Fig. 5. The effect of contact time on the adsorption of molybdate anion on resins.

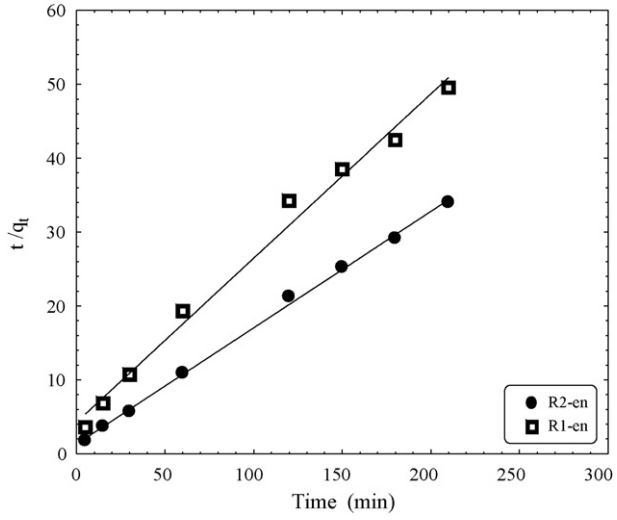

Fig. 6. Pseudo-second-order kinetic plots of the adsorption of molybdate anion on resins.

Table 3
Parameters of pseudo-second-order kinetics for the adsorption of molybdate anion from initial concentration of 8×10^{-3} M on the resins

Resin	q_e (exp.) (mmol/g)	q_e (theo.) (mmol/g)	k_2 (g/mmol min)	Correlation coefficient (R^2)
R1-en	4.24	4.50	0.011	0.9882
R2-en	6.18	6.35	0.019	0.9983

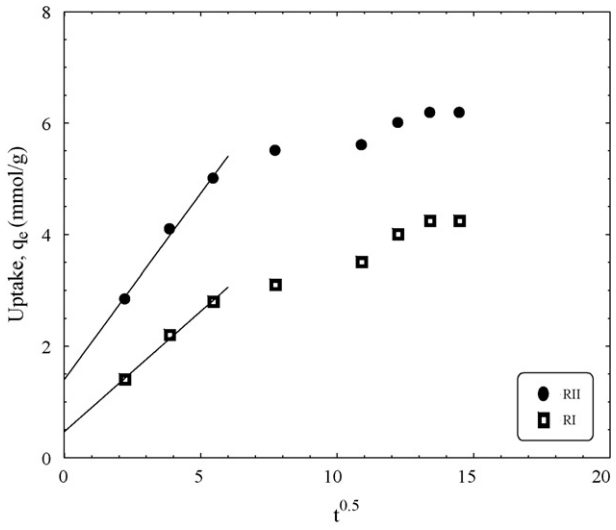

Fig. 7. The intraparticle diffusion kinetics model of the uptake of molybdate anion by the studied resins as Mo(VI) at 28 °C and pH 2.

5. Column studies

The features of the applicability of the resins for recovery of molybdate anion in flow systems were verified from studying effect of flow rate and resin bed height on the breakthrough.

5.1. Effect of flow rate

The breakthrough curves of the studied resin towards adsorption of molybdate anion at different flow rates (1, 2 and 3 mL/min) and a fixed bed height of 2 cm are shown in Fig. 8. It is noticed that the breakthrough and exhaustion of both resins occur faster at higher flow rates. At the same bed height and a flow rate of 1 mL/min, the breakthrough points of R1-en and R2-en resins are 285 and 440 min, respectively. The longer breakthrough time of R2-en may be related to its higher uptake capacity as well as higher binding constant value (K_{ads}) relative to those of R1-en. This behavior indicates the higher efficiency of R2-en for the removal of molybdate anion relative to R1-en.

5.2. Effect of bed height

The effect of bed height on the breakthrough time in Fig. 9, the bed height was varied from 1 to 3 cm while the flow rate was held constant at 1 mL/min. The effect of bed height was checked in terms of breakthrough time (t_b) and service time (t_s). Generally, both values increase with the increase in bed height. This indicates that the efficiency of removal of both resins is positively affected by the bed height. The critical bed height was obtained from bed depth service time model (BDST) which states that bed height (Z) and service time (t_s) of the column shows a linear relationship according to the relation [39]:

$$t_s = \frac{N_o Z}{C_o \upsilon} - \frac{1}{K_a C_o} \ln\left(\frac{C_o}{C_t} - 1\right). \quad (10)$$

where C_t is the concentration of the metal ion at the saturation time just prior the initial concentration C_o (i.e. $C_o/C_t = 100/99$),

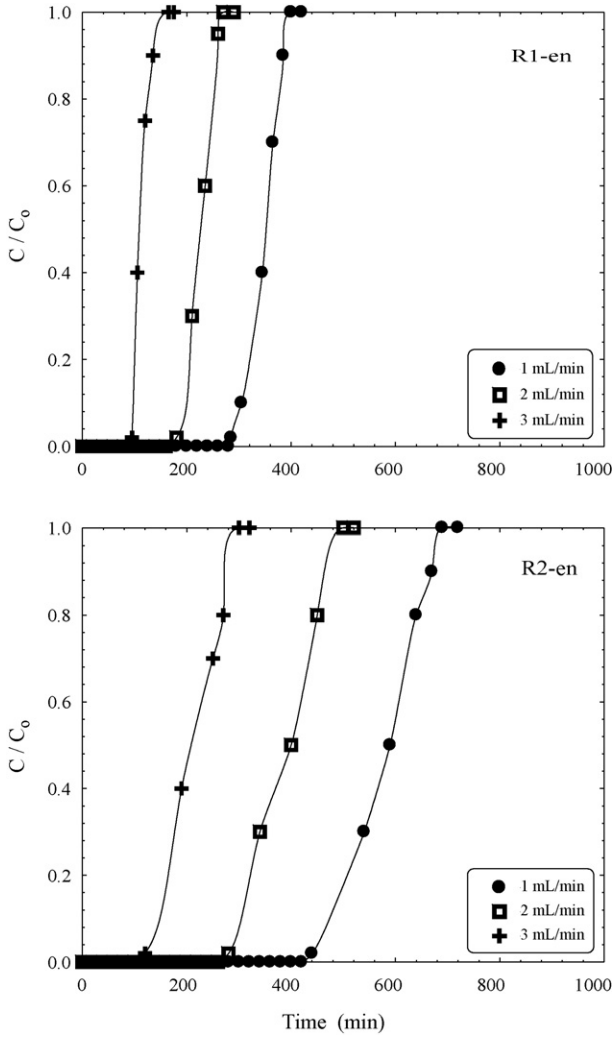

Fig. 8. Effect of flow rate on the uptake of molybdate anion by resins.

N_o the total adsorption capacity (mmol solute/L of sorbent bed), υ the linear velocity (cm/min) and K_a the rate constant of transfer (L/mmol min). The values of N_o and K_a were calculated from the slope and intercept of the BDST plots in Fig. 10. The calculated values of N_o for the resins were found to be 4 and 6 mmol/g for R1-en and R2-en, respectively. These values are comparable with the experimental values of Q_{max} at 28 °C Table 1. This indicates the validity of BDST model for the investigated resins. The values of K_a obtained for R1-en and R2-en were found to be 30.6 and 76.5 L/mmol min, respectively. The higher value of K_a implies that a shorter bed height is sufficient to delay the breakthrough. The critical bed height (Z_o) can be calculated by setting $t_s = 0$ in Eq. (10) and rearranging to get [39]:

$$Z_o = \frac{\upsilon}{K_a C_o} \ln\left(\frac{C_o}{C_b} - 1\right). \quad (11)$$

where C_b is the breakthrough metal ion concentration (mmol/L). The above equation implies that Z_o depends on the kinetics of the adsorption process, the residence time of the solute and the adsorption capacity of the resin. The critical bed height of R1-en and R2-en were found to be 0.05 and 0.01 cm. These values again

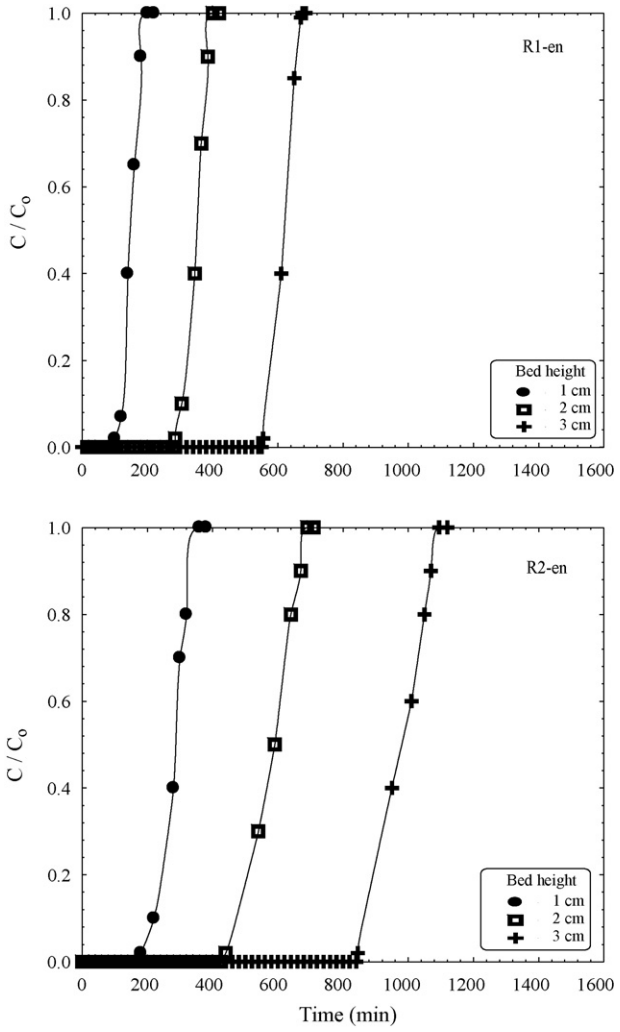

Fig. 9. Effect of bed height on the uptake of molybdate anion by resins.

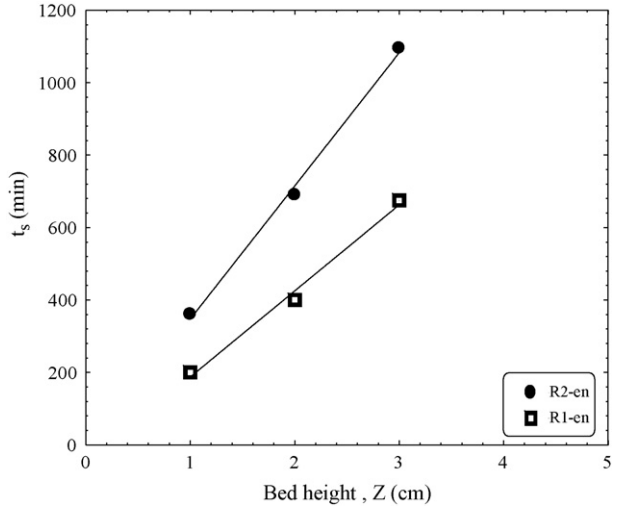

Fig. 10. Variation of service time (t_s) with the bed height of resins.

confirm the higher efficiency of R2-en than R1-en for molybdate removal.

6. Resin regeneration

Regeneration of the resins was carried out using a mixture of 0.1 M ammonium hydroxide and 0.01 M ammonium chloride. The regeneration of the resins may be represented as:

$$2\text{R-NH}_3{}^+\text{X}^- + \text{NH}_4\text{OH}/\text{NH}_4\text{Cl} = 2\text{R-NH}_2 + \text{NH}_4\text{X} + \text{HCl} + \text{H}_2\text{O} \quad (12)$$

where X is the adsorbed anion. The regeneration efficiency was found to be 96 and 90% for R1-en and R2-en resins, respectively over three cycles with a standard deviation of ± 0.5. The regeneration efficiencies are related to the Langmuir binding constant values, Table 1. As the value of the binding constant increases, the elution efficiency decreases.

7. Conclusion

Magnetic resins derived from glycidyl methacrylate and croslinked with divinylbenzen or *N*,*N*′-methylenebisacrylamide were prepared. The two resins were anchored with tetraethylenepentamine as active moieties. The presence of a hydrophilic crosslinker promoted the uptake properties of the resin towards molybdate anion. The maximum uptake of molybdate anion was found to be 6.18 mmol/g for R2-en resin at 28 °C This value is considered high compared to that early reported by others, 0.4 mmol/g [16]. The adsorption of molybdate anion on both resins was found to proceed according to pseudo-second-order kinetics indicating the influence of textural properties of resin on the rate of adsorption. The thermodynamic parameters obtained showed that the adsorption process is endothermic and dominated by entropy rather than enthalpy change.

References

[1] M. Harsfall Jr., A.I. Spiff, Effects of temperature on the sorption of Pb^{2+} and Cd^{2+} from aqueous solution by caladium bicolor (Wild Cocoyam) biomass, Electron. J. Biotechnol. 8 (2) (2005) 162–169.
[2] B.C. Bostick, S. Fendorf, G.R. Helz, Differential adsorption of molybdate and tetrathiomolybdate on pyrite (FeS2), Environ. Sci. Technol. 37 (2) (2003) 285–291.
[3] D. Malinovsky, I. Rodushkin, D.C. Baxter, J. Ingri, B. Ohlander, Molybdenum isotope ratio measurements on geological samples by MC-ICPMS, J. Mass Spectrom. 245 (2005) 94–107.
[4] K.C. Emregul, A.A. Aksut, The effect of sodium molybdate on the pitting corrosion of aluminum, J. Corros. Sci. 45 (2003) 2415–2433.
[5] G. Mu, X. Li, Q. Qu, J. Zhou, Molybdate, tungstate as corrosion inhibitors for cold rolling steel in hydrochloric acid solution, J. Corros. Sci. 48 (2006) 445–459.
[6] A. Moret, J. Rubio, Sulphate and molybdate ions uptake by chitin-based shrimp shells, Miner. Eng. 16 (2003) 715–722.
[7] C. Namasivayam, D. Sangeetha, Removal of molybdate from water by adsorption onto $ZnCl_2$ activated coir pith carbon, Bioresour. Technol. 97 (2006) 1194–1200.
[8] R. Mamtaz, D.H. Bache, Reduction of arsenic in groundwater by coprecipitation with iron, J. Water Supply: Res. Technol. AQUA 50 (2001) 313–324.

[9] Y. Al-Wazzan, M. Safar, A. Mesri, Reverse osmosis brine staging treatment of subsurface water, Desalination 155 (2003) 141–151.
[10] Y. Zhao, J.S. Taylor, S. Chellam, Predicting RO/NF water quality by modified solution diffusion model and artificial neural networks, J. Membr. Sci. 263 (2005) 38–46.
[11] P.J. Phelan, S.V. Maltigod, Adsorption of molybdate anion)$MoO4^{-2}$)by sodium-saturated kaolinite, Clays Clay Miner. 32 (1984) 45–48.
[12] H. Faghihian, A. Malekpour, M.G. Maragheh, Adsorption of molybdate ion by natrolite and clinoptolite-rich tuffs, Int. J. Environ. Pollut. 18 (2002) 181–189.
[13] J.P. Gustafsson, Modelling molybdate and tungstate adsorption to ferrihydrite, Chem. Geol. 200 (2003) 105–115.
[14] T. Fujita, G. Dodbiba, J. Sadaki, A. Shibayama, Removal of anionic metal ions from wastewater by hydroxide-type adsorbents, Chin. J. Process. Eng. 6 (2006) 357–362.
[15] K. Bourikasj, T. Hiemstra, W.H. Van Riemsdijk, Adsorption of molybdate monomers and polymers on titania with a multisite approach, J. Phys. Chem. B 105 (2001) 2393–2403.
[16] S. Goldberg, H.S. Forster, C.L. Godfrey, Molybdenum adsorption on oxides, clay minerals and soils, Soil Sci. Soc. Am. J. 60 (1996) 425–432.
[17] C.H. Wu, C.Y. Kuo, C.F. Lin, S.L. Lo, Modeling competitive adsorption of molybdate, sulfate, selenate and selenite using a Freundlich-type multicomponent isotherm, Chemosphere 47 (2002) 283–292.
[18] B.L. Rivas, H.A. Maturana, P. Hauser, Adsorption behavior and separation of vanadium(V), molybdenum(VI), and rhenium(VII) ions on crosslinked polymers containing acrylic acid derivative moieties, J. Appl. Polym. Sci. 73 (1999) 369–376.
[19] A.A. Atia, A.M. Donia, K.Z. Elwakeel, Adsorption behaviour of non-transition metal ions on a synthetic chelating resin bearing iminoacetate functions, Sep. Purif. Technol. 43 (2005) 43–48.
[20] A.A. Atia, A.M. Donia, K.Z. Elwakeel, Selective separation of mercury(II) using a synthetic resin containing amino and mercaptan as chelating groups, React. Funct. Polym. 65 (2005) 267–275.
[21] A.A Atia, A.M. Donia, A.M. Yousif, Synthesis of amine and thio chelating resins and study of their interaction with zinc(II), cadmium(II) and mercury(II) ions in their aqueous solutions, React. Funct. Polym. 56 (2003) 75–82.
[22] A.A. Atia, A.M. Donia, A.M. Yousif, Comparative study on the recovery of silver(I) from aqueous solutions using different chelating resins derived from glycidyl methacrylate, J. Appl. Polym. Sci. 97 (3) (2005) 806–816.
[23] A.A Atia, A.M. Donia, S.A. Abou-Ei-Enein, A.M. Yousif, Studies on uptake behaviour of copper(II) and lead(II) by amine chelating resins with different textural properties, Sep. Purif. Technol. 33 (2003) 295–301.
[24] D. Horak, N. Semenyuk, F. Lednicky, Effect of reaction parameters on the particle size in the dispersion polymerization of 2-hydroxyethyl and glycidyl methacrylate in the presence of a ferrofluid, J. Polym. Sci., Part A; Polym. Chem. 41 (2003) 1848–1863.
[25] N. Bicak, D.C. Sherrington, S. Sungur, N. Tan, A glycidyl methacrylate based resin with pendant urea groups as a high capacity mercury specific sorbent, React. Funct. Polym. 54 (2003) 141–147.
[26] A. Nastasovic, S. Jovanovic, D. Dordevic, A. Onjia, D. Jakovljevic, T. Novakovic, Metal sorption on macroporous poly(GMA-co-EGDMA) modified with ethylene diamine, React. Funct. Polym. 58 (2004) 139–147.
[27] D. Horak, N. Benedyk, Magnetic poly(glycidyl methacrylate) microspheres prepared by dispersion polymerization in the presence of electrostatically stabilized ferrofluids, J. Polym. Sci. Part A; Polym. Chem. 42 (2004) 5827–5837.
[28] A.A. Atia, A.M. Donia, A.E. Shahin, Studies on the uptake behavior of a magnetic Co_3O_4-containing resin for Ni(II), Cu(II) and Hg(II) from their aqueous solutions, Sep. Purif. Technol. 46 (2005) 208–213.
[29] A.M. Donia, A.A. Atia, H. El-Boraey, D.H. Mabrouk, Uptake studies of copper(II) on glycidyl methacrylate chelating resin containing Fe_2O_3 particles, Sep. Purif. Technol. 49 (2006) 64–70.
[30] M. Yamaura, R.L. Camilo, M.C.F.C. Felinto, Synthesis and performance of organic-coated magnetite particles, J. Alloys Compd. 344 (2002) 152–156.
[31] A.A Atia, A.M. Donia, S.A. El-Enein, A.M. Yousif, Effect of chain length of aliphatic amines immobilized on a magnetic glycidyl methacrylate resin towards the uptake behavior of Hg(II) from aqueous solutions, Sep. Sci. Technol. 42 (2007) 403–420.
[32] Y.K. Sun, M. Ma, Y. Zhang, N. Gu, Synthesis of nanometer-size maghemite particles from magnetite, Colloids Surf. A 245 (2004) 15–19.
[33] F. Will, J.H. Yoe, Colorimetric determination of molybdenum with mercaptoacetic acid, Anal. Chem. 25 (9) (1953) 1363–1366.
[34] S.S. Tahir, N. Rauf, Thermodynamic studies of Ni(II) adsorption onto bentonite from aqueous solution, J. Chem. Thermod. 35 (2003) 2003–2009.
[35] V.K. Gupta, P. Singh, N. Rahman, Adsorption behavior of Hg(II), Pb(II) and Cd(II) from aqueous solution on duolite C-433: a synthetic resin, J. Colloid Interf. Sci. 275 (2004) 398–402.
[36] A.M. Donia, A.A. Atia, H.A. El-Boraey, D.H. Mabrouk, Adsorption of Ag(I) on glycidyl methacrylate/*N*,*N*'-methylene bis-acrylamide chelating resins with embedded iron oxide, Sep. Purif. Technol. 48 (2006) 281–287.
[37] Y.S. Ho, G. McKay, Pseudo-second order model for sorption processes, Process Biochem. 34 (1999) 451–465.
[38] L. Krim, S. Nacer, G. Bilango, Kinetics of chromium sorption on biomass fungi from aqueous solution, Am. J. Environ. Sci. 2 (1) (2006) 31–36.
[39] K. Vijayaraghavan, J. Jegan, K. Palanivelu, M. Velan, Bioadsorption of cobalt(II) and nickel(II) by seaweeds: batch and column studies, Sep. Purif. Technol. 44 (1) (2005) 53–59.